Exploring Singlet Fission with *Ab initio* methods

Hanna Cho

January, 2024

Contents

The review looks into quantum information science and various *ab initio* methods to explore potential applications of the singlet fission process.

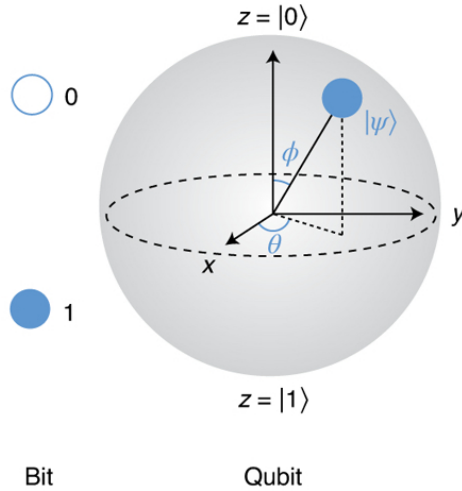# 1 Quantum Information Background

Figure 1: A comparison between a classical bit and a qubit.[1].

A qubit is a two-level system, similar to the classical bit. Just as bits serve as the basic unit of information in classical computing, qubits are the information unit in quantum information science. Figure 1 describes the bit and qubit. The Bloch sphere is the Hilbert space of the two-level system mapped in 3D space. By parameterizing with θ and ϕ as shown in Figure 1, the qubit state can be expressed as eq (1). While bits are binary and exist in only one of two states, 0 and 1, qubits can exist simultaneously in multiple states. For example, as shown in eq (1), state Ψ exists simultaneously in both $|0\rangle$ and $|1\rangle$ states. This phenomenon is referred to as the superposition state[2].

$$|\Psi\rangle = \cos\frac{\theta}{2}|0\rangle + e^{i\phi}\sin\frac{\theta}{2}|1\rangle. \tag{1}$$

Measurement in quantum systems is probabilistic, where the probability of a state being measured is the square modulus of the coefficients associated with that state. Therefore, the probabilities of observing outcomes $|0\rangle$ and $|1\rangle$ are $|\cos\frac{\theta}{2}|^2$ and $|\sin\frac{\theta}{2}|^2$, respectively, and the sum of all probabilities equals 1. Furthermore, the outcome state of measurement is always normalized, a phenomenon often referred to as the wave function collapse.

Processing of quantum information includes understanding the evolution of the quantum states. The time-dependent Schrödinger equation (TDSE), as shown in Equation (2), describes these dynamics, analogous to how Newton's second law characterizes the motion of classical objects. In this equation, $\hbar$ denotes the Planck constant, $|\Psi(t)\rangle$ represents an abstract state vector at time t. $\hat{H}$ is the Hamiltonian, a Hermitian operator corresponding to the total energy of the system.

$$i\hbar\frac{\partial}{\partial t}|\Psi(t)\rangle = \hat{H}|\Psi(t)\rangle. \tag{2}$$

Typically, solving this equation involves finding a unitary, evolution operator $u(t, t_0)$, enabling us to express the wave function at a specific time with $u(t, t_0)$ and the initial state $|\Psi(0)\rangle$. When the Hamiltonian is time-independent or commutes with itself at all times, the operator can easily be expressed as $u(t, t_0) = e^{-iHt}$. However, in a more general case with a time-dependent Hamiltonian, techniques such as transformation and approximation can be used. Plugging in the state expressed with the evolution operator, as shown in equations (3), it is easy to find that the TDSE can then be written without the state at a specific time.

$$i\hbar\dot{u}|\Psi(0)\rangle = \hat{H}u|\Psi(0)\rangle \quad\Rightarrow\quad i\hbar\dot{u} = \hat{H}u \ , \ u(t_0, t_0) = I. \tag{3}$$

An electron can be considered as a qubit with an intrinsic two-level system: spin up and spin down. When an electron is under the influence of processing magnetic fields, the total Hamiltonian for a single electron in position space is given by equation (4). The first term corresponds to the kinetic energy, and the second term corresponds to the potential energy. The third term, the Zeeman Hamiltonian, accounts for the effect of the external magnetic field, where μ_B represents the Bohr magneton, g characterizes the material's response anisotropy to the magnetic field, and $\vec{S}$ is the spin operators (the sum of all x, y, z spin operators), given by $\hat{S} = \hat{S}^x + \hat{S}^y + \hat{S}^z$. The position and time are separable, and on a basis where the spatial part is the energy eigenfunction, then the time-dependent Schrödinger equation (TDSE) can be written with the spin part carrying all time dependency and energy as a constant.

$$\hat{H} = -\frac{1}{2m}\nabla^2 + V(\vec{r}) + g\mu_B \vec{B} \cdot \vec{S} \tag{4}$$

Because the Hamiltonian is time-dependent, finding the unitary operator is not straightforward. However, through approximations and changes of basis, a new Hamiltonian can be defined to be time-independent. The unitary operator can then be expressed using the exponential of the Hamiltonian, which can be expanded with a Taylor series, or the Hamiltonian can be diagonalized so that the diagonal elements directly correspond to the exponents.

The Pauli matrices, as defined by eq (5), are Hermitian, unitary, and valuable concepts to know. The eigenstates of Pauli matrices align with the axes of the Bloch sphere, having eigenvalues of 1 and -1. The computational basis states, such as $|0\rangle$ and $|1\rangle$, previously used to express qubit states, are situated at the tip of the Z-axis. These states are orthogonal and represent the eigenstates of the Pauli Z operator.

$$\sigma_x = X = \begin{pmatrix} 0 & 1 \\ 1 & 0 \end{pmatrix}, \quad \sigma_y = Y = \begin{pmatrix} 0 & -i \\ i & 0 \end{pmatrix}, \quad \sigma_z = Z = \begin{pmatrix} 1 & 0 \\ 0 & -1 \end{pmatrix}. \tag{5}$$

Any two-level Hamiltonian can be expressed as a linear combination of Pauli matrices, and therefore, any spin operators can be as well. If the spin state is known, taking the expectation value of the Pauli matrices ($\sigma_x, \sigma_y, \sigma_z$) with respect to the state gives the spin vector representation. Then, the state is visually evident on the Bloch sphere, and the actions of qubit gates can be intuitively understood. For example, applying the σ_z gate to a $|0\rangle$ state induces a rotation by $\psi = \pi$ radians, effectively transforming it into $|1\rangle$.

Once the states are defined with parameters, we can find gates with parameters that give a probability of the desired state being 1. In the case of a single electron in a processing magnetic field with Hamiltonian as eq (4), the problem is well known as the Rabi problem in physics, analytically solvable to get the evolution operator, and gates from the evolution operator[3]. For example, evolution operator in lab frame is $u(t) = e^{i\frac{wt}{2}\sigma_z}e^{-i\frac{\lambda t}{2}\sigma_\theta}$. Such that the σ_z gate can then be obtained by finding frequency that gives a transition probability $\langle 1| u(t) |0\rangle$ equal to 1 which is $\lambda = \sqrt{\Omega_0^2 + \Delta^2}$ at time $\tau = \frac{\pi}{\Omega_0}$.

Quantum entanglement occurs when qubits are correlated, and the state of each qubit cannot be considered independently. This phenomenon is crucial for quantum computing and various technologies, including applications in quantum algorithms[4–6]. The correlations of entangled states persist even across long distances[7]. When a two-qubit state is not entangled, the total state can be written as a tensor product of individual states, $|\psi\rangle = |0\rangle_A |1\rangle_B$. The Hadamard and CNOT gates are well-established examples of quantum gates that generate entanglement, defined in equations (6). When these gates act on a separable state $|\psi\rangle$, the outcome is an entangled state. There are other two-qubit gates such as SWAP, Controlled Not(CNot), Controlled Z(CZ), Toffoli, and so on.

$$\text{Hadamard (H)} = \frac{1}{\sqrt{2}} \begin{pmatrix} 1 & 1 \\ 1 & -1 \end{pmatrix}, \qquad \text{CNOT} = \begin{pmatrix} 1 & 0 & 0 & 0 \\ 0 & 1 & 0 & 0 \\ 0 & 0 & 0 & 1 \\ 0 & 0 & 1 & \end{pmatrix}. \tag{6}$$

The density operator, $\rho = |\psi\rangle \langle\psi|$, provides an alternative representation of quantum states. Its diagonal elements indicate probabilities, with values ranging between 0 and 1, with the trace of 1 as the summation of all possibilities, which collectively equals 1. Much like the Schrödinger equation serves to address the time evolution of quantum systems, we employ evolution operators to describe how the density operator evolves. The equation of motion of the density matrix is often called the Liouvill-von Neumann equation shown in eq 7.

$$\frac{d\rho}{dt} = -\frac{i}{\hbar}[H, \rho]. \tag{7}$$

In nature, nothing exists alone, a system is constantly exposed to and entangled with its surrounding environment. In such a case, we can express the total Hamiltonian as the sum of the Hamiltonian of the system H_S and the environment H_B, and the interacting Hamiltonian between them H_{SB}. The jump operator, also called the Lindblad operator, L_i explains the evolution of the diagonal (relaxation) and off-diagonal (decoherence) elements of the Hamiltonian. The equation of motion of the open quantum system is modeled with the Lindblad Equation, expressed with the density matrix, total Hamiltonian, and the Jump operator shown as eq (8),[8][9]. The measure of qubit 'coherence' time is T_2, the inverse of the relaxation rate $1/2\gamma$, can be obtained from the Lindblad Equation[10][11].

$$\dot{\rho} = i[\rho, H_S + H_B + H_{SB}] = i[\rho, H] + \sum_i (L_i \rho L_i^\dagger - \frac{1}{2} L_i^\dagger L_i \rho - \frac{1}{2} \rho L_i^\dagger L_i) \tag{8}$$

The conditions necessary for a physical system to function as a qubit source are well-defined with five essential criteria[12]. These conditions include the system's capability to prepare qubits in a known state, scalability, and the necessity for long coherence times to facilitate effective control and provide reliable readout capability.

The Loss-DiVincenzo quantum computer concept utilizes a single electron as a qubit[13]. The electron is confined in 3D space with electrostatic potential. The Pauli operators are directly mapped with the spin states. The spin dynamic, then, can be explained with the total Hamiltonian consisting of the Heisenberg exchange Hamiltonian, eq (9), and the single electron Zeeman Hamiltonian as eq (4). The $\hat{S}_i \hat{S}_j$ is called a Heisenberg interaction, and J is the exchange coupling, arising from Coulomb interaction and the antisymmetric nature of fermions. The exchange coupling is often where theoretical calculations and experiments are compared. Zeeman terms provide single-qubit control, and two-qubit control is possible by adjusting the exchange coupling with magnetic fields.

$$\hat{H} = -\sum_{ij} J_{ij} \hat{S}_i \hat{S}_j + \sum_i g_i \mu_B \vec{B}_i \cdot \vec{S}_i \tag{9}$$

Molecules offer high potential, leveraging chemistry's capability for bottom-up design and possible modifications to exploit magnetic, optical, electronic, and many other properties[11,14–17]. While numerous experimental works have shown applications, there remains room for exploration in understanding the molecules. Additionally, beyond the benefits of quantum information technology, studying molecular dynamics and gaining a deeper understanding can contribute significantly to progress in chemistry

2 Quantum Chemistry: *Ab Initio* Methods

However, as discussed in Section 1 regarding qubit systems with electrons, solving the Hamiltonian is challenging even for the single-electron case. For systems with three or more electrons, considering all possible interactions becomes essential. A molecule comprises numerous atoms, each containing multiple subatomic particles, including electrons. Therefore, in addition to the multitude of variables and the complexity of the equations, the sheer dimension of the Hamiltonian required to account for all possible configurations is already too large to solve with simple calculations. Quantum chemistry has made significant progress in addressing such challenges. *Ab initio* methods, also known as wave function methods, aim to solve the Schrödinger equation from the beginning, constructing approximate wave functions based on the positions of nuclei and the number of electrons.

For simplicity, let's consider the time-independent Schrödinger equation (TISE), as shown in equations 10, with a simplified electronic Hamiltonian depicted in equations 11. Assuming that the potential associated with the system is time-independent, we can apply the Born-Oppenheimer approximation, which assumes that the electrons move much faster than the nuclei; we can treat the nuclear coordinates as fixed. In this simplification, hyperfine interactions are ignored, and the electronic states depend on electrons and parametrically on nuclear coordinates.

$$\hat{H}\left|\Psi\right\rangle = E\left|\Psi\right\rangle \tag{10}$$

$$\hat{H}(r, R) = -\sum_{i=1}^{N} \frac{1}{2}\nabla_i^2 - \sum_{i=1}^{N}\sum_{A=1}^{M} \frac{Z_A}{r_{iA}} + \sum_{i=1}^{N}\sum_{j>i}^{N} \frac{1}{r_{ij}} \tag{11}$$

2.1 Slater determinant

In the simplified electronic Hamiltonian shown in equations 11, a single electron's behavior is described by its spatial wavefunction, $\phi(r)$, where r includes Cartesian coordinates x, y, z, and its spin state, denoted by w (either α or β). A spin-orbital, denoted as $\chi(r, w)$, combines spatial and spin coordinates as a product of functions. For a system of N non-interacting electrons distributed across K atomic orbitals, the Hamiltonian can be represented as the sum of single-electron Hamiltonians for individual electrons. The eigenfunction of this system is a product of spin orbitals for each electron, known as the Hartree product and denoted as Ψ^{HP}

$$\Psi^{HP}(x_1, x_2, \cdots, x_N) = \chi_i(x_1)\chi_j(x_2)\cdots\chi_k(x_N) \tag{12}$$

Electrons follow the Pauli exclusion principle, where the electronic wave functions must exhibit antisymmetry upon the exchange of any two particles. This antisymmetric property can be achieved with the Slater determinant, $\left|\Psi^{SD}\right\rangle$, as shown in eq (13). The Slater determinant is defined as a linear combination of Hartree products, mathematically expressed in terms of matrix determinants. It is the simplest antisymmetric wave function that can describe the ground state of an N-electron system.

$$\left|\Psi^{SD}\right\rangle = \frac{1}{\sqrt{N!}} \begin{vmatrix} \chi_i(x_1) & \cdots & \chi_k(x_1) \\ \vdots & \ddots & \vdots \\ \chi_i(x_N) & \cdots & \chi_k(x_N) \end{vmatrix} = |\chi_i\chi_j\cdots\rangle \tag{13}$$

2.2 Hartree-Fock Method

The Hartree-Fock (HF) approach is the starting point for many *ab initio* methods. It provides an approximation to the many-body problems posed by an N-electron system through single-particle

states such that the solution can be a single Slater determinant. The single-particle states, $\{\chi_i\}$, can be chosen to be orthonormal. Then, using Lagrange's method of undetermined multipliers, with the constraint of orthonormality between spin orbitals and differentiating with respect to the molecular coefficients, it minimizes the expectation value of the Hamiltonian, providing the optimal set of orbitals with the lowest energy, ϵ_{ij} following eq (14).

$$\sum_i \epsilon_{ij}\chi_i(1) = \left[\hat{h} + \sum_j \int dx_2 \chi_j(2)\frac{1}{r_{12}}\chi_j(2) - \sum_j \int dx_2 \chi_j(2)\frac{1}{r_{12}}\hat{\mathcal{P}}\chi_j(2)\right]\chi_i(1) \tag{14}$$

Here, $\hat{\mathcal{P}}$ is an operator that interchanges electrons, for example, $\hat{\mathcal{P}}\chi_j(2)\chi_i(1) = \chi_i(2)\chi_j(1)$. Hartree-Fock (HF) is a mean-field method that captures the electron-electron interaction between the i-th and j-th electrons as an average potential from the other electrons. The second term in the second part of eq (14) accounts for the Coulombic interaction, while the third term accounts for the exchange interaction arising from the antisymmetric nature of fermions. Therefore, we can define the Fock operator ($\hat{f}$), which combines the kinetic and potential energies of electrons as described by the singlet electron Hamiltonian ($\hat{h}$), along with operators for the Coulombic interactions between electrons ($\hat{J}$) and the exchange interactions ($\hat{K}$). For electron k, eq (14) in terms of operators is written as follows:

$$\hat{f}(k) = \hat{h}(k) + \sum_{j=1}^{N}(\hat{J}_j(k) - \hat{K}_j(k)) \tag{15}$$

$$\hat{J}_j(1) = \sum_j \int dx_2 \chi_j^*(2)\frac{1}{r_{12}}\chi_j(2) \tag{16}$$

$$\hat{K}_j(1) = \sum_j \int dx_2 \chi_j^*(2) \frac{1}{r_{12}} \hat{\mathcal{P}} \chi_j(2) \tag{17}$$

The Roothaan-Hall formulation introduces a basis set by expanding the unknown molecular orbitals as a linear combination of a finite number of known atomic orbital basis functions $\{\phi_\mu\}$ with expansion coefficients c, as shown in equation 18. This formulation transforms the equation into a simple linear algebra problem. The resulting Fock matrix (F), overlap matrix (S), and matrix of expansion coefficients (c) solve the generalized eigenvalue equation, eq (19)

$$\chi_k = \sum_\mu c_{\mu k} \phi_\mu. \tag{18}$$

$$Fc = ESc. \tag{19}$$

Solving this matrix equation provides the optimal set of molecular orbitals and energies as eq (14). However, the Fock matrix depends on the density matrix, which relies on the basis set and molecular coefficients. Therefore, the self-consistent field (SCF) method is employed as an iterative approach. This method begins with a defined molecular geometry and a specified basis set, initiates with an initial guess of expansion coefficients, and iteratively updates the coefficients by diagonalizing the Fock matrix until the density matrix converges with the previous density matrix.

The computational cost of the HF scales is $O(N^4)$ owing to the two-electron integral calculations for N number of basis functions. However, in practice, many terms of two-electron integrals are small because of the small overlap between the orbitals. The cost can be reduced by performing screening techniques and density fitting to $O(N^3)$ [18,19]. The solution of the HF equations provides the electronic energy, electronic wave function, orbitals, and orbital energies.

When dealing with large molecular systems, the computational cost of diagonalization becomes

problematic. In such cases, the density-based HF offers an alternative approach. It circumvents the diagonalization steps by directly optimizing the one-electron density matrix under the atomic orbital (AO) basis. This method involves only the multiplication and addition of AO matrices, which are generally sparse, resulting in a linear scaling of the computational cost for large systems.

2.3   Correlation treatment

The Hartree-Fock (HF) procedure offers an approximation to the ground state, providing a zeroth-order wave function as a starting point for improvement. Post-Hartree-Fock methods were developed to address correlations, often categorized into two types: dynamical correlations arising from Coulomb repulsion and static correlations arising from near-degenerate states. These methods use a single determinant wave function as a reference ground state.

2.3.1   Configuration Interaction (CI)

The configuration Interaction (CI) methods involve a linear combination of different Slater determinants. The Full CI wave function, as depicted in eq (20), encompasses linear combinations of all possible configurations and is therefore considered an exact solution within a given basis set. Here, Ψ_0 represents the ground state wave function, while Ψ_i^a denotes determinants within the Fock space with singly excited states, achieved by switching the ith orbital with the ath orbital.

$$\left| \Psi^{FCI} \right\rangle = c_0 \left| \Psi^{(0)} \right\rangle + \sum_{i,a} c_i^a \left| \Psi_i^a \right\rangle + \sum_{ijab} c_{ij}^{ab} \left| \Psi_{ij}^{ab} \right\rangle + ... \tag{20}$$

Similar to the HF, the total CI wave functions are set to be orthonormal to each other; using a Lagrange multiplier with this constraint, the CI energy is to be obtained variationally. By optimizing expansion coefficients, one can lower the energy below the HF energy. Matrix elements can be evaluated with Slater's rule, and the matrix representation of the CI equation becomes eq (21)

where the solution is equivalent to the diagonalization of the CI matrix.

$$Hc = ESc \qquad (21)$$

Conceptually, Configuration Interaction is the simplest method. However, when dealing with $2K$ spin orbitals and N electrons, the size of the Full CI space equals the total number of configurations, encompassing the ground state, singly excited states, and more, resulting in a large combinatorial basis. For instance, with four orbitals and two electrons, there are 36 possible configurations, and the scaling is factorial with the number of configurations. In practice, truncated CI methods are often applied due to this computational challenge. Common truncations include CISD (truncated after single and double excitations). The scaling for CI methods is CISD ($\mathcal{O}(N^6)$), and CISD(T) is $\mathcal{O}(N^8)$. While the full CI method is size-consistent, truncated CI methods lose this property. Another crucial aspect of the CI method is its size-extensivity, where the energy of a system increases linearly with the number of electrons. If a method lacks size-extensivity, errors will grow as the size of the system increases.

2.3.2 Perturbation Theory

Another useful approach is perturbation theory. It assumes that the exact solution of a problem is only slightly different from a problem already solved. In perturbation theory, the Hamiltonian can be split into parts, with the easier-to-solve parts acting as the reference and the more challenging parts serving as the perturbation. The Hamiltonian can be written as:

$$\hat{H} = \hat{H}^{(0)} + \lambda \hat{H}^{(1)} \qquad (22)$$

Here, λ is an order parameter that tracks the significance of terms. In Møller-Plesset (MP)

perturbation theory, the Hartree-Fock (HF) ground state serves as the reference state. The zeroth-order Hamiltonian $\hat{H}^{(0)}$ is the Hartree-Fock Hamiltonian, and corrections are introduced in the perturbed terms $\hat{H}^{(1)}$, which include missing correlation from the Hartree-Fock method[20]. Then, the HF wave function and energies can be expanded using a Taylor series in λ :

$$|\Psi_i\rangle = \left|\Psi_i^{(0)}\right\rangle + \lambda \left|\Psi_i^{(1)}\right\rangle + \lambda^2 \left|\Psi_i^{(2)}\right\rangle + \cdots \tag{23}$$

$$E_i = E_i^{(0)} + \lambda E_i^{(1)} + \lambda^2 E_i^{(2)} + \cdots \tag{24}$$

Substituting eq (22),23 and 24 in eq (10) and collecting terms with the same order parameter λ, we obtain the perturbation equations. Multiplying the left side of the equation with the wave function of the desired order and arranging it with the order parameter λ gives the following correction energies. Second-order energy is shown in eq (25).

$$2^{nd} \text{ Order:} \quad E_i^{(2)} = \sum_{i \neq j} \frac{\left\langle \Psi_i^{(0)} \right| \hat{H}^{(1)} \left| \Psi_j^{(1)} \right\rangle \left\langle \Psi_i^{(1)} \right| \hat{H}^{(1)} \left| \Psi_j^{(0)} \right\rangle}{(E_i^{(0)} - E_j^{(0)})} \tag{25}$$

While perturbation methods are not variational and come with high computational costs (the formal scaling for MP2 methods goes as $O(N^5)$)[21–24], they can be effectively combined with other methods, improves the calculations by accounting the dynamic electron correlation. For example, CIS(D) combines Configuration Interaction Singles (CIS) with a correction using MP2, achieving accurate excited-state energies[25].

2.3.3 Coupled-cluster theory

Describing strongly correlated systems, where multiple Slater determinants contribute significantly to the exact wave function, poses a challenge known as static correlation. An illustrative example of this challenge is the Hartree-Fock (HF) reference of the H_2 molecule as its bond is stretched. The bonding orbital (σ) and antibonding orbital (σ^*) approach closer in energy as the distance between the nuclei increases. Ultimately, when the bond length becomes infinite, the σ^* and σ orbitals exhibit the same degenerate energy.

While both truncated CI methods and perturbative methods tend to perform poorly in these strongly correlated systems, coupled cluster theory involves all correlations by expanding the wave function, which is written as an exponential ansatz. The reference wave function is typically the Hartree-Fock (HF) molecular orbitals $\left| \Psi^{(0)} \right\rangle$, as shown in Equation (26)[26].

$$e^{\hat{T}} \left| \Psi^{(0)} \right\rangle = e^{\hat{T}_1 + \hat{T}_2 + \cdots} \left| \Psi^{(0)} \right\rangle \tag{26}$$

The exponential coupled cluster operators represent excitations in higher orbitals in sequential orders, with the first operator counting all single excitations and the second operator incorporating all double excitations and so on. Utilizing second quantization formalism, the operator can be expressed as in Equation (27).

$$\hat{T} = \hat{T}_1 + \hat{T}_2 + \cdots = \sum_{ia} t_i^a a_a^\dagger a_i + \frac{1}{4} \sum_{ijab} t_{ij}^{ab} a_a^\dagger a_b^\dagger a_j a_i + \ldots \tag{27}$$

The energy expectation value, written as $\left\langle \Psi_0 \right| e^{\hat{T}} \hat{H} e^{\hat{T}} \left| \Psi_0 \right\rangle = E$, can be evaluated using the Baker–Campbell–Hausdorff formula (BCH formula)[27]. This formula decomposes the product of two operators into a series of nested commutators, allowing the approximation of non-commuting operators as:

$$\bar{A}\bar{B} = e^{\hat{A}}\hat{B}e^{-\hat{A}} = \hat{B} + [\hat{A}, \hat{B}] + \frac{1}{2!}[[\hat{A}, \hat{B}], \hat{B}] + \dots$$

where $\hat{A}$ and $\hat{B}$ are operators, and $[.,.]$ denotes the commutator. This formulation allows for the derivation of the effective Hamiltonian for coupled cluster methods, as shown in equation (28):

$$\bar{H} = e^{-\hat{T}}\hat{H}e^{\hat{T}} = H + [H, T] + \frac{1}{2!}[[H, T], T] + \dots \tag{28}$$

The cluster operator $\hat{T}$ can be truncated similarly to the configuration interaction (CI) method to ensure computational efficiency. For example, in CCSD (coupled cluster with singles and doubles), only $\hat{T}_1$ and $\hat{T}_2$ terms remain in the exponential expansion[28]. The computational scaling of CCSD and CCSDT is $O(N^6)$ and $O(N^8)$, respectively[29]. CCSD(T), which incorporates the estimation of triples via perturbation theory, scales as $O(N^7)$ and is considered the standard method for achieving chemical accuracy. While coupled cluster theory is not variational, it is size-extensive and can describe electron correlation in the ground state.

2.3.4   Multi-configuration methods

Active space methods not only provide a well-established solution for static correlation problems but also enhance computational efficiency. By partitioning the orbitals into three distinct spaces, calculations can exclusively focus on the relevant orbitals. The classification of these spaces determines the specific approach utilized.

Complete Active Space (CAS) and Restricted Active Space (RAS) Methods: The Complete Active Space (CAS) methods partition the orbital space into three subspaces[30]. The core space consists of orbitals that consistently accommodate two electrons, while the virtual space comprises exclusively empty (virtual) orbitals. Full Configuration Interaction (Full CI) is employed to solve

all possible configurations formed within the specified set of active space orbitals. When the active space encompasses all orbitals, it is equivalent to Full Configuration Interaction (FCI); conversely, when there are no orbitals in the active space, it yields the Hartree-Fock wave function. However, the number of Configuration State Functions (CSFs) in the active space scales factorially with the number of electrons and orbitals in the active space [31].

Different derivatives exist depending on the method used to calculate in the active space, such as CASSCF and CAS-CI. In CASSCF, all orbitals can be relaxed upon iteration to minimize the energy. In CAS-CI, on the other hand, orbitals are fixed, and the minimal energy of the desired state is then calculated by variationally optimizing the expansion coefficients of the linear combinations of Slater determinants. However, current computing limits calculations to systems with fewer than 20 electrons in 20 orbitals. In addition to computational limits, it is still not sufficient to explain strongly correlated systems such as conjugated molecules, transition metal oxides, or conducting materials [32,33].

Active space can be doubly, singly occupied, or unoccupied. When changing the occupancy upon excitation or de-excitation, we need to consider the spin completeness. However, if the wave function describing a molecular system fails to properly account for the conservation of spin symmetry, leading to inaccuracies in the computed electronic properties, spin contamination arises. In CASSCF, spin contamination can occur due to improper mixing of determinants with different spin states, potentially leading to erroneous results, especially in systems with open-shell electronic configurations.

To mitigate spin contamination in CASSCF calculations, various techniques, such as spin projection methods or state-specific approaches, are employed. These methods aim to ensure the correct treatment of spin symmetry, thus improving the accuracy of electronic structure predictions in complex molecular systems. Addressing spin contamination is crucial for obtaining reliable insights into chemical reactivity, molecular properties, and reaction mechanisms in quantum

chemical simulations.

Restricted Active Space (RAS) methods, analogous to CAS, further improve efficiency compared to CAS methods. They partition the active orbitals into three subspaces: RAS1 holds doubly occupied orbitals, with electrons in RAS1 space capable of being excited into RAS2 and RAS3 spaces. RAS3 holds unoccupied orbitals, allowing holes in RAS3 space to take excitations from RAS1 and RAS2 spaces. The RAS2 subspace mirrors the CAS active space, allowing for all possible configurations[34,35]. While RAS methods offer efficiency compared to CAS methods, they can still be impractical with a large number of orbitals in space.

The Restricted Active Space-Spin Flip (RAS-SF) method is variational and excludes orbital optimization, making it faster than CAS methods. While the computational cost increases exponentially with a growing number of spin flips, it remains size-extensive with a moderate number of fixed spins. By performing Full CI in the active space, it achieves size-consistency, representing a rare example of a truncated CI method. However, it still faces a high computational cost when applied to large systems, as the number of possible configurations increases combinatorially with the number of spin-flip excitations corresponding to the number of chromophores.

3 Singlet fission for Quantum information science

A system of particular interest is a singlet fission process, a singlet excited state generating two triplet states observed in organic materials. It has been studied for more than 50 years and has recently gained more attention for its potential application of multiple exciton generation in energy science, overcoming the Shockley-Queisser limit, the thermodynamic limit up to 33% for power conversion efficiency in solar cells[36–38].

$$S_1 S_0 \; \rightleftharpoons \; {}^1(TT) \; \rightleftharpoons \; T_1 + T_1 \tag{29}$$
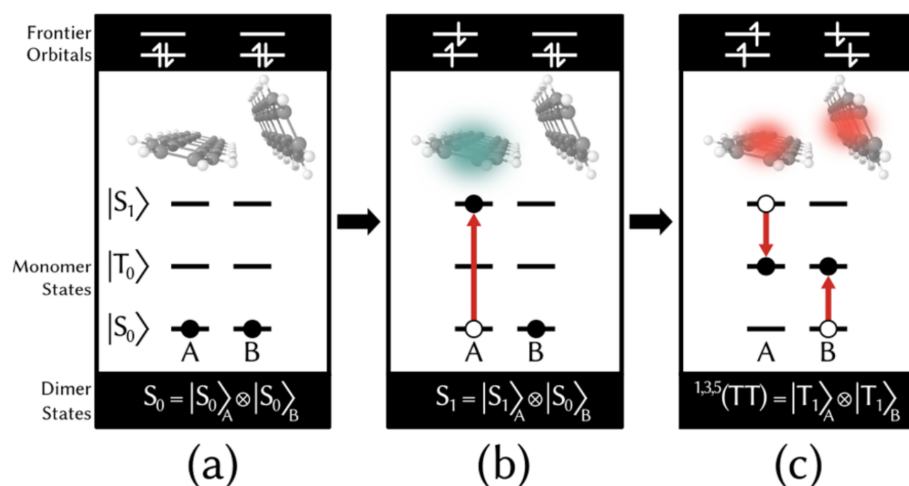
Figure 2: A basic mechanism of the singlet fission. (a) Ground state: Two molecules, A and B, each have paired electrons in the ground state. (b) Singly excited state: Absorption of energy from a photon excites one of the ground state electrons. (c) Biexciton state: correlated triplet pair excited state. By Nicholas M.[39]

Early works on photophysics and experiments suggested a kinetic model begins with molecules in the ground state S_0S_0 absorbing light and becoming excited, forming the initial singlet state S_0S_1. Subsequently, it transitions into a coupled singlet, correlated triplet state $^1(TT)$, which later evolves into two independent triplet states, $T+T$. The initial singlet state often exhibits strong fluorescence and is thus sometimes called the bright state, investigated through time-resolved fluorescence (TRF) experiments as far back as the 1960s[40][41]. The correlated triplet pair state, $^1(TT)$, is an intermediate pair state with an overall spin multiplicity of one, making the whole process spin-allowed. The existence of coupled triplet states was confirmed by observing delays in their fluorescence activity with varying energy levels[42]. Novel methods, including transient absorption (TA) spectra[43] and time-resolved electronic spin resonance (tr-EPR)[44] have been employed and confirmed the existence of entangled spin states even at room temperature, the magnetic effects, and the dynamics of singlet fission, pushing forward the study of singlet fission[17,45–48].

Figure 2 illustrates the singlet fission process in its simplest model with only HOMO/LUMO, the frontier orbitals, depicting a diagram from the ground state to a correlated triplet pair in each

electronic state. Potential applications in quantum information science could arise from the quintet state of singlet fission as a qudit[16,49], offering a possible implementation of Grover's algorithm on a molecular magnet[50]. The correlated triplet states decay highly selectively, making them particularly suitable for quantum information science. For example, with the Wigner-Eckhart theorem, we know that only ^{1}TT and ^{5}TT are possible[51,52]. The recent discovery of a quintet state ^{5}(TT) exhibiting a long time scale, even at room temperature[16,17,53], has brought significance to quantum information science.

As we have seen in Section1 and Section2, the theoretical study offers valuable insights into the electronic structures, underlying mechanisms, and dynamics of the singlet fission process. Zimmerman et al. utilized *ab initio* methods, employing multi-reference CASSCF to handle static correlation and treating dynamic correlation with second-order perturbation to the CASSCF[54], even before the experimental discovery. The complicated steps of the process were investigated with electronic structure theory, revealing charge transfer (CT) and charge resonance (CR) states[55][56]. Various potential transformation mechanisms from the initial excited state to a correlated triplet pair were suggested, including direct internal conversion[42], pathways mediated by CT states[57], and coherent transfer with CT intermediates[36,58,59].

Diagonalization of time-independent molecular Hamiltonian (eq 11) yields eigenstates on an adiabatic basis. These states are commonly employed in theoretical studies as they straightforwardly construct electronic states. However, it is important to note that adiabatic states do not change over time. Any time-dependent term, such as the time evolution of the nuclear wavefunction, should be described with derivative couplings between electronic states.

To account for these changes over time, the total wave function can be expressed using this complete set of adiabatic states. The diabatic states can also be defined with changing nuclei coordinates[60–62]. Another way of defining diabatic states is similar to adiabatic approximation in section 1, where with time-independent or commuting Hamiltonian, the diabatic states can be

constructed through the rotation of adiabatic eigenstates[63]. In diabatic basis, states are coupled only through the electronic Hamiltonian, which does not diagonalize the Hamiltonian anymore[62,64,65].

Alternatively, we can use the spin Hamiltonian, eq (9), to get an accurate description of the system with diabatic states. Considering only the correlated pair state with four-orbital, four-spin basis, Figure 2(c), there are 16 different possible spin configurations by distributing α and β spins. In a basis to obtain simultaneous eigenstates of S_z and S^2, a coupled state with total spin angular momentum (eigenvalue of S^2) of one gives mixed spin states, five quintet states, three triplet states, and one singlet state[66], which matches with historical assumptions in molecular photochemistry[67].

The resulting correlated pair states of 0 eigenvalues from S_z are shown in eq (30). S_i is the total spin of each molecule, $\mathbf{S}$ is the total spin of the dimer, and M_s is a projection of the total spin of the dimer onto the z-axis. The uncoupled states, $|m_i, s_i\rangle |m_j, s_j\rangle$ where the first state is the state of molecule A and the second state is the state of molecule B. The correlated pair, $^1(TT)$, is a superposition of three possible triplet states (where the total spin of a molecule is always one, but the projection onto the z-axis can be -1,0,1). Note that $^1(TT)$ is a pure state, the density matrix of this state is idempotent, and $\mathrm{Tr}(\rho^2) = 1$[66][68].

$$
\begin{aligned}
^1(TT) &\approx |S_1 = 1, S_2 = 1; \mathbf{S} = 0, M_S = 0\rangle \\
&= \frac{1}{\sqrt{3}} \left(|-1, 1\rangle |1, 1\rangle + |1, 1\rangle |-1, 1\rangle - |0, 1\rangle |0, 1\rangle \right)
\end{aligned}
\tag{30}
$$

$$
\begin{aligned}
^3(TT) &\approx |S_1 = 1, S_2 = 1; \mathbf{S} = 1, M_S = 0\rangle \\
&= \frac{1}{\sqrt{2}} \left(|-1, 1\rangle |1, 1\rangle - |1, 1\rangle |-1, 1\rangle \right)
\end{aligned}
\tag{31}
$$

$$
\begin{aligned}
^5(TT) &\approx |S_1 = 1, S_2 = 1; \mathbf{S} = 2, M_S = 0\rangle \\
&= \frac{1}{\sqrt{6}} \left(|-1, 1\rangle |1, 1\rangle + |1, 1\rangle |-1, 1\rangle + 2|0, 1\rangle |0, 1\rangle \right)
\end{aligned}
\tag{32}
$$

Analyzing the spin Hamiltonian provides the diabatic electronic states, exchange interactions between molecules, triplet transfer, or the energy transfer rate. This helps reveal potential new designs for molecules with modified properties, such as longer coherence time or higher efficiency, achieved by optimizing energetic conditions and geometry[69–71]. Magnetic effects and other dynamical values can be assessed by utilizing model Hamiltonians[72].

The operation of qubits typically involves the use of external magnetic or optical fields. Magnetic field-driven operations can be susceptible to disruption from thermal noise while inducing population inversion with optical fields poses challenges[44,73,74]. The singlet fission process involves both optical and magnetic experiments, resembling the behavior of the nitrogen-vacancy center in a diamond. As a molecular system, the potential for bottom-up design and modification of moieties enables the exploitation of magnetic, optical, electronic, and many other properties[10,11,75,76].

4   Research goals

The goal of my research is to utilize *ab initio* methods to investigate excited states in singlet fission, a process of interest for its potential applications in quantum information science. By employing computational techniques, we aim to gain insights into the underlying electronic structure and dynamics involved in singlet fission reactions.

In a recent study, the electron paramagnetic resonance (EPR) spectra associated with singlet fission were successfully calculated, and the dynamics were studied using the JDE model. This model incorporates parameters such as J (the inter-chromophore isotropic exchange coupling), D (intra-chromophore zero-field splitting axial parameter), and E (rhombicity parameter). These parameters were derived from solving the model Hamiltonian with just HOMO and LUMO orbitals, as shown in equation (33), where s represents the regular electron spin operator and O_{ij} accounts for the spin-spin interaction. The study demonstrated the accurate prediction of magnetic sublevels

and highlighted the potential of EPR experiments as quantum gates for singlet fission materials.

$$H = \sum_{i,j}^{4} s_i \cdot O_{ij} \cdot s_j \tag{33}$$

Novel experimental investigations focusing on coherence time, decoherence mechanisms, and laser coupling need more theoretical studies. The total time-dependent density matrix $\rho(t)$ and the system-bath Hamiltonian H can be used to describe the system's evolution. If the density operator of states is well defined, the T_2 decoherence time and the decoherence rate could be measured and simulated[9,13]. Exact solutions for density equations have been using reduced density matrices (RDMs). However, the highly correlated nature of molecular systems and the complexity of the many electron interactions poses challenges. Accurate modeling and analysis require more advanced computational methods than active space techniques.

4.1   Implementation of *Ab initio* Methods for Singlet fission

Selection Of Active Space: The selection of the active space traditionally relied on chemical intuition or was often supplemented by insights from low-level methods and natural orbital analysis[77,78]. TDDFT have been utilized for this purpose. Although TDDFT may fail, especially with multi-excitonic states and extended pi molecules present during the singlet fission process. Computational methods such as CIS, TDHF, and the density embeddings could be used for calculation on specific orbitals to see where the correlation lies[79–82]. For instance, the energy of excited tetracene has been a subject of investigation in this context[37,83].

Tensor product selective configuration interaction   Various computational methods have been employed for studying the dynamics of singlet fission. These include spin-flip methods[84,85], where the occurrence of a single spin flip has been investigated[86,87]. Additionally, approaches involving

CIS and SOC have been explored[88]. Techniques such as TPSCI and DUCC have been implemented to understand the dynamics of specific systems like the tetracene dimer. Furthermore, investigations into the decoherence of triplet pair states have provided valuable insights into the underlying mechanisms.

Model Hamiltonian for the Singlet Fission Study: The study of singlet fission often involves the use of model Hamiltonians to elucidate the underlying mechanisms. These Hamiltonians are designed to capture the relevant electronic and spin interactions within the molecular system. Specific considerations are made for factors such as inter-chromophore coupling, zero-field splitting, and rhombicity. The development and refinement of such model Hamiltonians play a crucial role in advancing our understanding of singlet fission processes and their potential applications in various fields.

References

[1] Emani, P. S. et al. Quantum Computing at the Frontiers of Biological Sciences. *Nat. Methods* **2021**, *18*, 701–709.

[2] Nielsen, M. A.; Chuang, I. L. *Quantum Computation and Quantum Information*; Cambridge University Press, 2010.

[3] Paul, H. *Introduction to Quantum Optics: From Light Quanta to Quantum Teleportation*; Cambridge University Press: Cambridge, 2004.

[4] Kitaev, A. Y. Quantum measurements and the Abelian Stabilizer Problem. *arXiv:quant-ph/9511026* **1995**, Submitted on 20 Nov 1995.

[5] Castellanos, M. A.; Willard, A. P. Designing Excitonic Circuits for the Deutsch–Jozsa Algorithm: Mitigating Fidelity Loss by Merging Gate Operations. *23*, 15196–15208.

[6] Filidou, V.; Simmons, S.; Karlen, S. D.; Giustino, F.; Anderson, H. L.; Morton, J. J. L. Ultrafast Entangling Gates between Nuclear Spins Using Photoexcited Triplet States. **2012**, *8*, 596–600.

[7] Aspelmeyer, M.; Böhm, H. R.; Gyatso, T.; Jennewein, T.; Kaltenbaek, R.; Lindenthal, M.; Molina-Terriza, G.; Poppe, A.; Resch, K.; Taraba, M.; Ursin, R.; Walther, P.; Zeilinger, A. Long-Distance Free-Space Distribution of Quantum Entanglement. *Science* **2003**, *301*, 621–623.

[8] Lindblad, G. On the Generators of Quantum Dynamical Semigroups. *Communications in Mathematical Physics* **1976**, *48*, 119–130.

[9] Manzano, D. A short introduction to the Lindblad master equation. *AIP Advances* **2020**, *10*, 025106.

[10] Schlosshauer, M. Quantum Decoherence. **2019**, *831*, 1–57.

[11] Wasielewski, M. R. et al. Exploiting Chemistry and Molecular Systems for Quantum Information Science. **2020**, *4*, 490–504.

[12] DiVincenzo, D. P.; IBM, The Physical Implementation of Quantum Computation. **2000**, *48*, 771–783.

[13] Loss, D.; DiVincenzo, D. P. Quantum computation with quantum dots. *Phys. Rev. A* **1998**, *57*, 120–126.

[14] Zadrozny, J. M.; Niklas, J.; Poluektov, O. G.; Freedman, D. E. Millisecond Coherence Time in a Tunable Molecular Electronic Spin Qubit. *ACS Central Science* **2015**, *1*, 488–492.

[15] Atzori, M.; Sessoli, R. Title of the Article. *Journal of the American Chemical Society* **2019**, *141*, 11339–11352.

[16] Jacobberger, R. M.; Qiu, Y.; Williams, M. L.; Krzyaniak, M. D.; Wasielewski, M. R. Using Molecular Design to Enhance the Coherence Time of Quintet Multiexcitons Generated by Singlet Fission in Single Crystals. *J. Am. Chem. Soc.* **2022**, *144*, 2276–2283.

[17] Yamauchi, A., et al. Room-temperature quantum coherence of entangled multiexcitons in a metal-organic framework. *Sci. Adv.* **2024**, *10*, eadi3147.

[18] Whitten, J. L. Coulombic potential energy integrals and approximations. *J. Chem. Phys.* **1973**, *58*, 4496–4501.

[19] Werner, H.-J.; Manby, F. R.; Knowles, P. J. Fast linear scaling second-order Møller-Plesset perturbation theory (MP2) using local and density fitting approximations. *J. Chem. Phys.* **2003**, *118*, 8149.

[20] Møller, C.; Plesset, M. S. Note on an Approximation Treatment for Many-Electron Systems. *Phys. Rev.* **1934**, *46*, 618–622.

[21] Pulay, P.; Saebø, S. Theoret. Chim. Acta. **1986**, *69*, 357–368.

[22] Saebø, S.; Pulay, P. J. Chem. Phys. **1987**, *86*, 914–922.

[23] Jensen, F. *Introduction to Computational Chemistry*, 2nd ed.; Wiley, 2006.

[24] Cremer, D. Møller–Plesset Perturbation Theory: From Small Molecule Methods to Methods for Thousands of Atoms. *WIREs Comput Mol Sci* **2011**, *1*, 509–530.

[25] Head-Gordon, M.; Rico, R. J.; Oumi, M.; Lee, T. J. A Doubles Correction to Electronic Excited States from Configuration Interaction in the Space of Single Substitutions. **1994**, *219*, 21–29.

[26] Bartlett, R. J. Coupled-Cluster Approach to Molecular Structure and Spectra: A Step toward Predictive Quantum Chemistry. *J. Phys. Chem.* **1989**, *93*, 1697–1708.

[27] Van-Brunt, A.; Visser, M. Explicit Baker–Campbell–Hausdorff Expansions. *Mathematics* **2018**, *6*, 135.

[28] Purvis, G. D.; Bartlett, R. J. A full coupled-cluster singles and doubles model: The inclusion of disconnected triples. *The Journal of Chemical Physics* **1982**, *76*, 1910–1918.

[29] Crawford, T. D.; Schaefer, H. F. In *Reviews in Computational Chemistry*, 1st ed.; Lipkowitz, K. B., Boyd, D. B., Eds.; Wiley, 2000; Vol. 14; pp 33–136.

[30] Roos, B. O. The Complete Active Space Self-Consistent Field Method and its Applications in Electronic Structure Calculations. *Adv. Chem. Phys.* **2007**, *69*, 399–445.

[31] Andersson, K.; Malmqvist, P.; Roos, B. O. Second-Order Perturbation Theory with a Complete Active Space Self-Consistent Field Reference Function. *J. Chem. Phys.* **1992**, *96*, 1218–1226.

[32] Imada, M.; Fujimori, A.; Tokura, Y. Metal-Insulator Transitions. **1998**, *70*, 225.

[33] Soos, Z. G. Molecular Correlations and Neutral Excitations of Conjugated Polymers. **1994**, *256*, 35–44.

[34] Malmqvist, P. A.; Rendell, A.; Roos, B. O. The Restricted Active Space Self-Consistent-Field Method, Implemented with a Split Graph Unitary Group Approach. **1990**, *94*, 5477–5482.

[35] Carreras, A.; Jiang, H.; Pokhilko, P.; Krylov, A. I.; Zimmerman, P. M.; Casanova, D. Calculation of Spin–Orbit Couplings Using RASCI Spinless One-Particle Density Matrices: Theory and Applications. **2020**, *153*, 214107.

[36] Chan, W.-L.; Ligges, M.; Zhu, X. The energy barrier in singlet fission can be overcome through coherent coupling and entropic gain. *Nature Chemistry* **2012**, *4*, 840–845.

[37] Daiber, B.; Maiti, S.; Ferro, S. M.; Bodin, J.; van den Boom, A. F. J.; Luxembourg, S. L.; Kinge, S.; Pujari, S. P.; Zuilhof, H.; Siebbeles, L. D. A.; Ehrler, B. Change in Tetracene Polymorphism Facilitates Triplet Transfer in Singlet Fission-Sensitized Silicon Solar Cells. *The Journal of Physical Chemistry Letters* **2020**, *11*, 8703–8709.

[38] Tsuneda, T.; Taketsugu, T. Singlet Fission Initiating Organic Photosensitizations. *Sci Rep* **2024**, *14*, 829.

[39] Mayhall, N. J. From Model Hamiltonians to Ab Initio Hamiltonians and Back Again: Using Single Excitation Quantum Chemistry Methods To Find Multiexciton States in Singlet Fission Materials. *J. Chem. Theory Comput.* **2016**, *12*, 4263–4273.

[40] Merrifield, R. E. Magnetic Effects on Triplet Exciton Interactions. *Pure and Applied Chemistry* **1971**, *27*, 481–498.

[41] Johnson, R. C.; Merrifield, R. E. Effects of Magnetic Fields on the Mutual Annihilation of Triplet Excitons in Anthracene Crystals. *Phys. Rev. B* **1970**, *1*, 896–902.

[42] Burdett, J. J.; Bardeen, C. J. Quantum beats in crystalline tetracene delayed fluorescence due to triplet pair coherences produced by direct singlet fission. *Journal of the American Chemical Society* **2012**, *134*, 8597–8607.

[43] Pensack, R. D.; Ostroumov, E. E.; Tilley, A. J.; Mazza, S.; Grieco, C.; Thorley, K. J.; Asbury, J. B.; Seferos, D. S.; Anthony, J. E.; Scholes, G. D. Observation of Two Triplet-Pair Intermediates in Singlet Exciton Fission. *The Journal of Physical Chemistry Letters* **2016**, *7*, 2370–2375.

[44] Smyser, K. E.; Eaves, J. D. Singlet Fission for Quantum Information and Quantum Computing: The Parallel JDE Model. **2020**, *10*, 18480.

[45] Xu, R.; Zhang, C.; Xiao, M. Magnetic field effects on singlet fission dynamics. *J. Am. Chem. Soc.* **2022**, *144*, 1234–1245.

[46] Maity, N.; Kim, W.; Panjwani, N. A.; Kundu, A.; Majumder, K.; Kasetty, P.; Mishra, D.; Bittl, R.; Nagesh, J.; Dasgupta, J.; Musser, A. J.; Patil, S. Parallel Triplet Formation Pathways in a Singlet Fission Material. **2022**, *13*, 5244.

[47] MacDonald, T.; Tayebjee, M.; Collins, M.; Kumarasamy, E.; Sanders, S.; Sfeir, M.; et al., Anisotropic multiexciton quintet and triplet dynamics in singlet fission via PEANUT. *Chem-Rxiv* **2023**, This content is a preprint and has not been peer-reviewed.

[48] Neef, A.; Beaulieu, S.; Hammer, S.; et al., Orbital-resolved observation of singlet fission. *Nature* **2023**, *616*, 275–279.

[49] Ringbauer, M.; Meth, M.; Postler, L.; et al., A universal qudit quantum processor with trapped ions. *Nat. Phys.* **2022**, *18*, 1053–1057.

[50] Leuenberger, M.; Loss, D. Quantum computing in molecular magnets. *Nature* **2001**, *410*, 789–793.

[51] Edmonds, A. R. *Angular Momentum in Quantum Mechanics*; Princeton University Press, 1996; Revised edition.

[52] Sakurai, J. J.; Tuan, S. F. *Modern Quantum Mechanics*; Addison-Wesley Publishing Company: Reading, Mass., 1994; Revised edition.

[53] Collins, M. I.; Campaioli, F.; Tayebjee, M. J. Y.; et al., Quintet formation, exchange fluctuations, and the role of stochastic resonance in singlet fission. *Commun Phys* **2023**, *6*, 64.

[54] Zimmerman, P. M.; Zhang, Z.; Musgrave, C. B. Singlet Fission in Pentacene through Multi-Exciton Quantum States. **2010**, *2*, 648–652.

[55] Smith, M. B.; Michl, J. Recent Advances in Singlet Fission. *64*, 361–386.

[56] Cao, Y.; Romero, J.; Aspuru-Guzik, A. Potential of Quantum Computing for Drug Discovery. *IBM Journal of Research and Development* **2018**, *62*, 6:1–6:20.

[57] Monahan, N.; Zhu, X. Charge Transfer–Mediated Singlet Fission. *Annual Review of Physical Chemistry* **2015**, *66*, 601–618.

[58] Greyson, E. C.; Vura-Weis, J.; Michl, J.; Ratner, M. A. Maximizing Singlet Fission in Organic Dimers: Theoretical Investigation of Triplet Yield in the Regime of Localized Excitation and Fast Coherent Electron Transfer†. *The Journal of Physical Chemistry B* **2010**, *114*, 14168–14177.

[59] Li, X.; Parrish, R. M.; Martínez, T. J. An ab initio exciton model for singlet fission. *The Journal of Chemical Physics* **2020**, *153*, 184116.

[60] Subotnik, J. E.; Cave, R. J.; Steele, R. P.; Shenvi, N. The initial and final states of electron and energy transfer processes: Diabatization as motivated by system-solvent interactions. *The Journal of Chemical Physics* **2009**, *130*, 234102.

[61] Subotnik, J. E.; Vura-Weis, J.; Sodt, A. J.; Ratner, M. A. Predicting accurate electronic excitation transfer rates via Marcus theory with Boys or Edmiston-Ruedenberg localized diabatization. *Journal of Physical Chemistry A* **2010**, *114*, 8665–8675.

[62] Subotnik, J. E.; Alguire, E. C.; Ou, Q.; Landry, B. R.; Fatehi, S. The Requisite Electronic Structure Theory to Describe Photoexcited Nonadiabatic Dynamics: Nonadiabatic Derivative Couplings and Diabatic Electronic Couplings. *Acc. Chem. Res.* **2015**, *48*, 1340–1350.

[63] Sun, K.; Liu, X.; Hu, W.; Zhang, M.; Long, G.; Zhao, Y. Singlet fission dynamics and optical spectra of pentacene and its derivatives. *Phys. Chem. Chem. Phys.* **2021**, *23*, 12654–12667.

[64] Malhado, J. P.; Bearpark, M. J.; Hynes, J. T. Non-Adiabatic Dynamics Close to Conical Intersections and the Surface Hopping Perspective. *Front. Chem.* **2014**, *2*, 97.

[65] Shu, Y.; Varga, Z.; Kanchanakungwankul, S.; Zhang, L.; Truhlar, D. G. Diabatic States of Molecules. *J. Phys. Chem. A* **2022**, *126*, 992–1018.

[66] Scholes, G. D. Correlated Pair States Formed by Singlet Fission and Exciton-Exciton Annihilation. *J. Phys. Chem. A* **2015**, *119*, 12699–12705.

[67] Saltiel, J.; Atwater, B. W. Spin-Statistical Factors in Diffusion-Controlled Reactions. *Adv. Photochem.* **1988**, *14*, 1–90.

[68] Sanders, S. N.; Pun, A. B.; Parenti, K. R.; Kumarasamy, E.; Yablon, L. M.; Sfeir, M. Y.; Campos, L. M. Understanding the Bound Triplet-Pair State in Singlet Fission. *Chem* **2019**, *5*, 1988–2005.

[69] Tayebjee, M. J. Y.; Gray-Weale, A. A.; Schmidt, T. W. Thermodynamic Limit of Exciton Fission Solar Cell Efficiency. **2012**, *3*, 2749–2754.

[70] Buchanan, E. A.; Havlas, Z.; Michl, J. In *Advances in Quantum Chemistry*; Sabin, J. R., Brändas, E. J., Eds.; Academic Press, 2017; Vol. 75; pp 175–227.

[71] Lewis, S. G.; Smyser, K. E.; Eaves, J. D. Clock transitions guard against spin decoherence in singlet fission. *The Journal of Chemical Physics* **2021**, *155*, 194109.

[72] Abraham, V.; Mayhall, N. J. Revealing the Contest between Triplet–Triplet Exchange and Triplet–Triplet Energy Transfer Coupling in Correlated Triplet Pair States in Singlet Fission. **2021**, *12*, 10505–10514.

[73] Weil, J. A.; Bolton, J. R. *Electron Paramagnetic Resonance: Elementary Theory and Practical Applications*, 2nd ed.; Wiley, 2007.

[74] Niknam, M.; Chowdhury, M. F. F.; Rajib, M. M.; et al., Quantum control of spin qubits using nanomagnets. *Communications Physics* **2022**, *5*, 284.

[75] Gaita-Ariño, A.; Luis, F.; Hill, S.; et al., Molecular spins for quantum computation. *Nat. Chem.* **2019**, *11*, 301–309.

[76] Bayliss, S. L.; Laorenza, D. W.; Mintun, P. J.; Kovos, B. D.; Freedman, D. E.; Awschalom, D. D. Optically Addressable Molecular Spins for Quantum Information Processing. *370*, 1309–1312.

[77] Helbig, N.; Tokatly, I. V.; Rubio, A. Physical meaning of the natural orbitals: Analysis of exactly solvable models. *Phys. Rev. A* **2010**, *81*, 022504.

[78] Krylov, A. I. From orbitals to observables and back. *J. Chem. Phys.* **2020**, *153*, 080901.

[79] Dreuw, A.; Head-Gordon, M. Single-Reference Ab Initio Methods for the Calculation of Excited States of Large Molecules. **2005**, *105*, 4009–4037.

[80] Manby, F. R.; Stella, M.; Goodpaster, J. D.; Thomas F. Miller, I. A Simple, Exact Density-Functional-Theory Embedding Scheme. *J. Chem. Theory Comput.* **2012**, *8*, 2564–2568.

[81] Manby, F. R.; Stella, M.; Goodpaster, J. D.; Miller, I., Thomas F. A Simple, Exact Density-Functional-Theory Embedding Scheme. *J. Chem. Theory Comput.* **2015**, *11*, 2671–2685.

[82] Claudino, D.; Mayhall, N. J. Automatic Partition of Orbital Spaces Based on Singular Value Decomposition in the Context of Embedding Theories. *J. Chem. Theory Comput.* **2019**, *15*, 1053–1064.

[83] Casanova, D. Electronic Structure Study of Singlet Fission in Tetracene Derivatives. *Journal of Chemical Theory and Computation* **2014**, *10*, 324–334.

[84] Krylov, A. I. Spin-flip configuration interaction: an electronic structure model that is both variational and size-consistent. *Chemical Physics Letters* **2001**, *350*, 522–530.

[85] Casanova, D. Theoretical Modeling of Singlet Fission. **2018**, *118*, 7164–7207.

[86] Mayhall, N. J.; Head-Gordon, M. Computational quantum chemistry for single Heisenberg spin couplings made simple: Just one spin flip required. *J. Chem. Phys.* **2014**, *141*, 134111.

[87] Mayhall, N. J.; Head-Gordon, M. Computational Quantum Chemistry for Multiple-Site Heisenberg Spin Couplings Made Simple: Still Only One Spin–Flip Required. *J. Phys. Chem. Lett.* **2015**, *6*, 1982–1988.

[88] Bellonzi, N.; Medders, G. R.; Epifanovsky, E.; Subotnik, J. E. Configuration interaction singles with spin-orbit coupling: Constructing spin-adiabatic states and their analytical nuclear gradients. *J. Chem. Phys.* **2019**, *150*, 014106.